Archival Report

Biological Psychiatry

Genetic Mapping in Mice Reveals the Involvement of *Pcdh9* in Long-Term Social and Object Recognition and Sensorimotor Development

Hilgo Bruining, Asuka Matsui, Asami Oguro-Ando, René S. Kahn, Heleen M. van't Spijker, Guus Akkermans, Oliver Stiedl, Herman van Engeland, Bastijn Koopmans, Hein A. van Lith, Hugo Oppelaar, Liselotte Tieland, Lourens J. Nonkes, Takeshi Yagi, Ryosuke Kaneko, J. Peter H. Burbach, Nobuhiko Yamamoto, and Martien J. Kas

ABSTRACT

BACKGROUND: Quantitative genetic analysis of basic mouse behaviors is a powerful tool to identify novel genetic phenotypes contributing to neurobehavioral disorders. Here, we analyzed genetic contributions to single-trial, long-term social and nonsocial recognition and subsequently studied the functional impact of an identified candidate gene on behavioral development.

METHODS: Genetic mapping of single-trial social recognition was performed in chromosome substitution strains, a sophisticated tool for detecting quantitative trait loci (QTL) of complex traits. Follow-up occurred by generating and testing knockout (KO) mice of a selected QTL candidate gene. Functional characterization of these mice was performed through behavioral and neurological assessments across developmental stages and analyses of gene expression and brain morphology.

RESULTS: Chromosome substitution strain 14 mapping studies revealed an overlapping QTL related to long-term social and object recognition harboring *Pcdh9,* a cell-adhesion gene previously associated with autism spectrum disorder. Specific long-term social and object recognition deficits were confirmed in homozygous (KO) *Pcdh9*-deficient mice, while heterozygous mice only showed long-term social recognition impairment. The recognition deficits in KO mice were not associated with alterations in perception, multi-trial discrimination learning, sociability, behavioral flexibility, or fear memory. Rather, KO mice showed additional impairments in sensorimotor development reflected by early touch-evoked biting, rotarod performance, and sensory gating deficits. This profile emerged with structural changes in deep layers of sensory cortices, where *Pcdh9* is selectively expressed.

CONCLUSIONS: This behavior-to-gene study implicates *Pcdh9* in cognitive functions required for long-term social and nonsocial recognition. This role is supported by the involvement of *Pcdh9* in sensory cortex development and sensorimotor phenotypes.

Keywords: Associative learning, Autism spectrum disorder, Genetic mapping, Information processing, *Pcdh9*, QTL, Quantitative trait locus, Recognition, Sensory cortex, Social cognition

http://dx.doi.org/10.1016/j.biopsych.2015.01.017

The genetic architecture of psychiatric disorders is complex and composed of multiple interacting factors. Although many candidate genes have been identified, not much is known on how these genes impact specific components of behavior and social functioning (1,2). One of the reasons is the difficulty of linking gene products or molecular pathways to the expression of social behavior; another, the challenge to find meaningful genetic phenotypes that directly relate to cognitive deficits in human psychopathology. A commonly proposed solution to enhance the relevance and specificity of genetic phenotypes is to focus on underlying quantitative traits that more directly index neurobiological disruptions (3–5). This is an attractive approach, though highly demanding, requiring large human samples characterized for relevant phenotypes. To overcome this limitation, we have proposed a complementary strategy to perform quantitative genetic analysis of basic social behaviors in mice that are regulated by processes likely to be conserved across species (6). The advantage of this approach is that genetic variation underlying differences in specific traits can be detected using sophisticated mapping panels to gain understanding of brain function.

In this study, we followed this strategy and performed the first forward genetic screen of social recognition (SRE) in mice followed by a functional characterization of a candidate gene

ISSN: 0006-3223

in a newly generated knockout (KO) model. We chose SRE, as it represents a basic behavior to form social relationships and to establish social hierarchies essential for survival (7,8). Taking advantage of this, SRE tests provide a unique approach to test essential brain functions required for social behavioral adaptation. Social recognition can be analyzed in a social discrimination task that takes advantage of the innate drive of animals to investigate unfamiliar over familiar social stimuli and allows direct stimulus presentation for the acquisition of the full olfactory signature (9,10). This test is inexpensive and fast with easy application and therefore highly suitable for quantitative trait locus (QTL) studies involving large numbers of mice. The SRE capacity can be tested after one-trial learning with different time intervals, offering the unique opportunity to separately investigate different processes underlying recognition during social interaction (9). For instance, impairments in both short-term and long-term SRE may indicate inadequate sensory (e.g., smell) perception or basic encoding problems, while an impairment restricted to long-term but not short-term SRE indicates proper encoding but reduced consolidation or cognitive processing of social information. Impairments in such higher order processes will have consequences for long-term social interactions and may affect behavioral development. Furthermore, cue specificity of recognition can be investigated by comparing the performance in social versus nonsocial (object) discrimination (11).

Here, we describe the QTL mapping of social recognition in a panel of consomic strains, leading to the implication of protocadherin 9 (*Pcdh9*) in long-term social and object recognition and other phenotypes related to higher order information processing.

METHODS AND MATERIALS

Chromosome Substitution Strains

Breeding pairs for C57BL/6J, A/J, and all 21 C57BL/6J-Chr #^{A}/NaJ (chromosome substitution strain [CSS]) strains (# = 1–19, X or Y) were obtained from the Jackson Laboratory (Bar Harbor, Maine). Strain colonies were subsequently bred in-house. All experiments were approved by the ethical committee for animal experimentation of the University Medical Center Utrecht and performed according to the University Medical Center institutional guidelines that are in full compliance with the European Council Directive (86/609/EEC).

Social and Object Discrimination Tests

Two-day versions of social and object discrimination paradigms were used to measure social and object recognition capacity, as we performed previously (12) (Supplement 1). In brief, for social discrimination, test animals were habituated in the test cage for 5 minutes and initially exposed to an age- and gender-matched A/J conspecific for 2 minutes and then, after intertrial intervals (ITI) of 5 minutes, exposed to the familiar conspecific and a first novel A/J conspecific for 2 minutes. On day 2, after the 24-hour ITI, the test animal was habituated for 5 minutes and re-exposed to the same familiar intruder of day 1 and to a different novel intruder animal from a different cage and housing room than the intruder of day 1 for 2 minutes. For object discrimination, a similar test was used involving novel and familiar objects instead of intruder mice (Supplement 1). Behavioral assessments were conducted at 3 to 5 months of age and only male mice were used in the current study.

QTL Mapping

A CSS14-F_1 generation was derived by reciprocal mating of C57BL/6J and C57BL/6J-Chr 14^{A}/NaJ (CCS14) animals. The F_1 hybrids were intercrossed, producing CSS14-F_2 animals. The F_2 and control C57BL/6J animals were tested at the same age range as the CSS mice with social and object discrimination tests consecutively in fixed order, with 1 to 2 weeks between the tests. DNA samples of the CSS14-F_2 mice were obtained according to a standard procedure (13). For generating a genetic map of chromosome 14, 19 microsatellites were chosen from the mouse genome database (Mouse Genome Informatics, Jackson Laboratory, Bar Harbor, Maine; http://www.informatics.jax.org/) (Supplement 1). Segregation ratio of the genotypes of individual microsatellite markers was checked with the chi-squared goodness-of-fit test. None of the markers showed significant segregation distortion ($p > .05$). Cox *et al.* (14) have constructed a revised genetic map of the mouse genome and demonstrated that utilization of the revised map improves QTL mapping. Therefore, marker positions were taken from this map by using the mouse map converter (Jackson Laboratory; http://cgd.jax.org/mousemapconverter/). The location of the QTLs affecting the measured quantitative traits was determined by using the scan one function in the R/qtl package (http://www.R-project.org) and using cross as an additive and interactive covariate (15). Because the traits were normally distributed, the interval-mapping module was used. Results were expressed as logarithm of the odds (LOD) scores. The LOD score threshold level was determined through permutation tests (random shuffling of genotypes with phenotype based on 10,000 permutations). The LOD score threshold level, set at a confidence level of .05 (this level is generally accepted for statistical significance) was 3.31, whereas at tenfold, increased confidence level (.005) corresponds to a LOD score of 4.52. The power to detect a main effect locus was calculated using R/qtlDesign (http://www.R-project.org)(16). Based on an average marker density of $\sim$ 3.0 cM, 192 CSS14-F_2 mice are sufficient to detect a QTL that has a LOD score of 3.31 and accounting for 10% of the variance in the phenotypes with a power of 80%.

Generation and Breeding of *Pcdh9* Knockout Mice

Pcdh9-deficient mice were generated using a standard procedure (17) (Supplement 1). A targeting vector was designated to delete the second exon of the mouse *Pcdh9* gene, which encodes extracellular, transmembrane, and part of cytoplasmic domains (Supplement 1).

Developmental Behavioral and Neurological Screening

The extended SmithKline Beecham, Harwell, Imperial College, Royal London Hospital, phenotype assessment was used to assess basic sensorimotoric functions, locomotor activity, and various reflexes in mice (18,19) (Supplement 1). Sociability was measured using the three-chambered apparatus (20) and a variant of the reversal/set-shifting task was used to assess multi-trial discrimination learning and behavioral flexibility (12) (Supplement 1). Anxiety-like behavior in a novel environment

was measured in an open field test (Supplement 1). Fear-conditioning tests were performed in a computer-controlled fear-conditioning system (TSE-Systems, Bad Homburg, Germany) as described previously (21). Acoustic startle and prepulse inhibition (PPI) were measured during one 45-minute session as reported previously (21) (Supplement 1).

In Situ Hybridization Profiling of *Pcdh9* Expression

In situ hybridization was performed using a digoxigenin-labeled complementary RNA probe for a 5' untranslated region, according to a method described previously (Supplement 1).

Analysis of Cortical Thickness

Cortical thickness was assessed in primary somatosensory area (bregma −1.70 mm: primary somatosensory barrel cortex field) and primary visual area (bregma −2.30 mm) using 30-μm serial Nissl-stained brain sections at 100-μm intervals (Supplement 1).

Immunohistochemistry

Immunohistochemistry was performed on 30-μm serial coronal brain sections using NeuN primary antibody (Chemicon, Billerica, Massachusetts) and Foxp2 primary antibody (Chemicon) (Supplement 1).

Golgi Staining and Analysis

Golgi staining was performed on freshly dissected brains using a FD Rapid GolgiStain kit (FD NeuroTechnologies, Columbia, Maryland). Dendrites and dendritic spines in L6 of S1 were traced using Neurolucida software (MicroBrightField, Williston, Vermont).

Statistical Analysis

Statistical analyses were performed using SPSS 18.0 (Quarry Bay, Hong Kong) (for details, see Supplement 1).

RESULTS

Genetic Mapping of Long-Term Social and Object Recognition Capacity in Chromosome Substitution Strains

To map QTLs underlying SRE in mice, we tested the C57BL/6J-Chr#A/NaJ mouse CSS panel (22) as a genetic reference panel in a social discrimination paradigm. This consomic mapping panel has previously been used as a sensitive genetic reference panel to identify QTLs affecting behavioral processes (23–26). CSS mice were exposed to a familiar and an unfamiliar conspecific following a 5-minute short-term and 24-hour long-term ITI to investigate short-term and long-term SRE capacity (9). Variable SRE performance was observed among CSSs following these ITIs (Figure 1A,B). To detect QTLs specifically related to long-term recognition, the effect size of the difference between 5-minute and 24-hour ITI recognition indices (Cohen's d = [Mean_5 min − Mean_24 h]/[pooled standard deviation]) was analyzed to select CSS

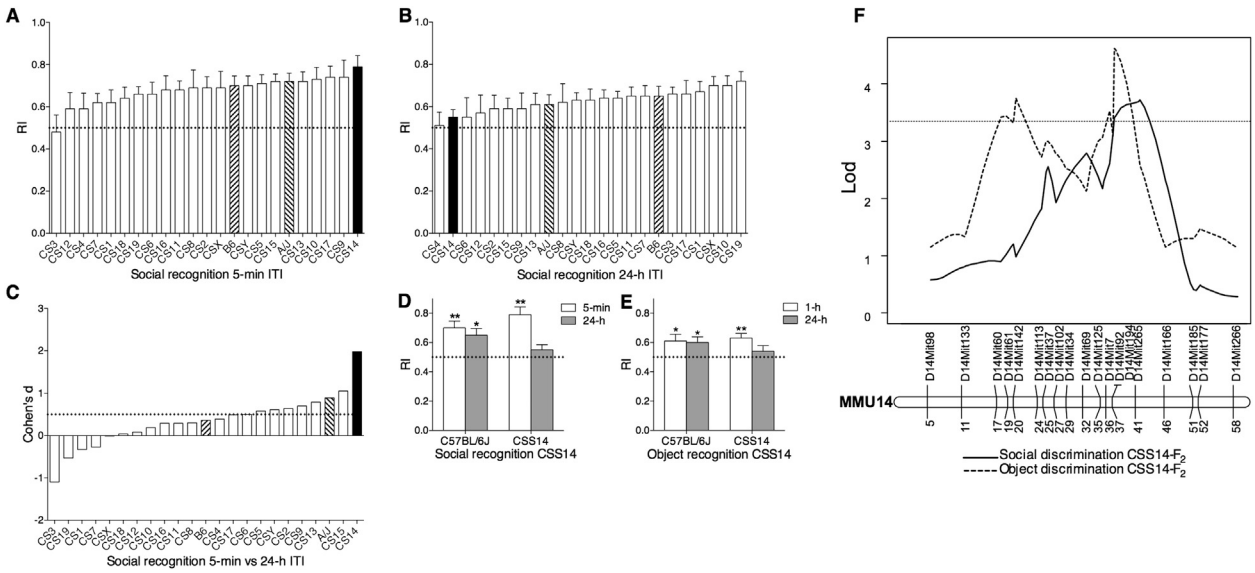

Figure 1. Quantitative trait locus mapping of social and object recognition using chromosome substitution strains. **(A,B)** Social recognition (SRE) in the chromosome substitution strain (CSS) panel (n = 8 per CSS) after 5-minute **(A)** and 24-hour **(B)** intertrial interval (ITI). Recognition index (RI)—values higher than .5 (dotted line)—indicate that test mice spent more time investigating the unfamiliar intruder compared with the familiar intruder. Most strains displayed significant increase of social recognition ratio above chance (recognition index greater than .5) following the 5-minute ITI, apart from three CSS (CSS3, CSS4, and CSS12) . In contrast, five CSS (CSS4, CSS6, CSS9, CSS14, and CSS15) did not show significant SRE after 24-hour ITI or impairments in both ITIs (e.g., CSS4 and CSS12). **(C)** The effect size of the difference between social recognition after 5-minute and 24-hour ITI. **(D,E)** Short-term and long-term social **(D)** and object recognition **(E)** assessments in C57BL/6J and the selected CSS14 with impaired long-term social and object recognition but intact short-term performance. **(F)** Logarithm of the odds (LOD) score plot for social recognition index (solid line) and object recognition index (dotted line) for performance after 24-hour ITI in the CSS14-F_2 population (n = 192). The dashed horizontal line represents the threshold value (3.31) of the LOD score considered significant for linkage. Genetic map (lower panel) of mouse chromosome 14 (MMU14) (the male revised Shifman map). Data are presented as the mean ± SEM; $^*p < .05$, $^{**}p < .01$.

strains for further genetic mapping (Figure 1C). Accordingly, CSS14 was selected as the strain with impaired long-term SRE and the strongest decrease in SRE from 5-minute to 24-hour ITI. We further analyzed associated behaviors in CSS14 during the social interaction sessions and found no significant differences in the duration of social exploration, activity, rearing, autogrooming, and immobility between this strain and the C57BL/6J control animals in any of the test trials, including during habituation. Thus, the differences in long-term recognition were not associated with social avoidance, reduced sociability, or exploratory behaviors (data not shown). To establish if the long-term SRE impairment of CSS14 (Figure 1D) was limited to social cues, we also analyzed novel object recognition (NORE) capacity. Similar to SRE, CSS14 showed intact NORE following short-term ITI but impaired NORE following the long-term ITI (Figure 1E).

To localize genetic loci on chromosome 14 that are associated with SRE and NORE capacity, an F_2 progeny of 192 male mice (derived from an F_1 intercross of C57BL/6J-Chr 14^A/NaJ X C57BL/6J hybrids) was tested in the social and object discrimination paradigms used for CSS14. Following phenotyping and genotyping of the F_2 animals, QTL analysis on the CSS14-F_2 population revealed significant LOD scores for both long-term SRE and NORE, while no significant LOD scores were obtained following the short-term SRE or NORE. One chromosomal segment was mapped for SRE following 24-hour ITI and two segments were mapped for NORE following the 24-hour ITI (Figure 1F). Furthermore, no significance was reached for other phenotypes, such as locomotor activity levels, exploration time, or rearing behavior. The highest peak for SRE had a LOD score of 3.72 with a 1.0 LOD support interval of 90,927,318-106,412,167 base pair that showed a partial 5.5 Mb overlap with the second QTL segment linked to 24-hour ITI NORE performance, covering 92,453,717-97,908,061 base pair. These QTLs accounted for 11.0% and 11.1% of the variance in the long-term SRE and NORE capacity in the F_2 population, respectively. This overlapping locus indicated the presence of genes regulating long-term SRE and NORE after single trial exposure.

Selection of *Pcdh9* as a Candidate Gene from the QTL Analysis

To pinpoint candidate genes contributing to long-term recognition performance in the overlapping 5.5-Mb QTL region, we scrutinized genes and genetic variations using the following selection criteria: 1) brain expression, 2) protein variants coded by one or more nonsynonymous single nucleotide polymorphisms (nsSNPs) (with http://www.jax.org/) between the progenitor strains of the CSS panel (A/J and C57BL/6J), and 3) evidence for association with neurodevelopmental disorders from human genetic studies. Following this procedure (Supplement 1), we revealed nsSNPs in two genes with predominant brain expression: kelch-like 1 (*Klhl1*) and protocadherin 9 (*Pcdh9*). *Pcdh9* was selected as a promising candidate in the QTL region because *Pcdh9*, a member of the cadherin subfamily of protocadherins, is implicated in brain development and functioning (27,28). Multiple members of this large cell-adhesion protein family display strong and localized expression in the nervous system (29–31) and have been implicated in a variety of neurodevelopmental disorders (29,32,33). A particular association of *PCDH9* with autism spectrum disorder (ASD) has been suggested by de novo and inherited copy number variation, both deletions and duplications, and was further supported by the finding of downregulated transcript levels in lymphoblasts of ASD patients (34–38). Furthermore, *PCDH9* has also been associated with social behavioral traits in

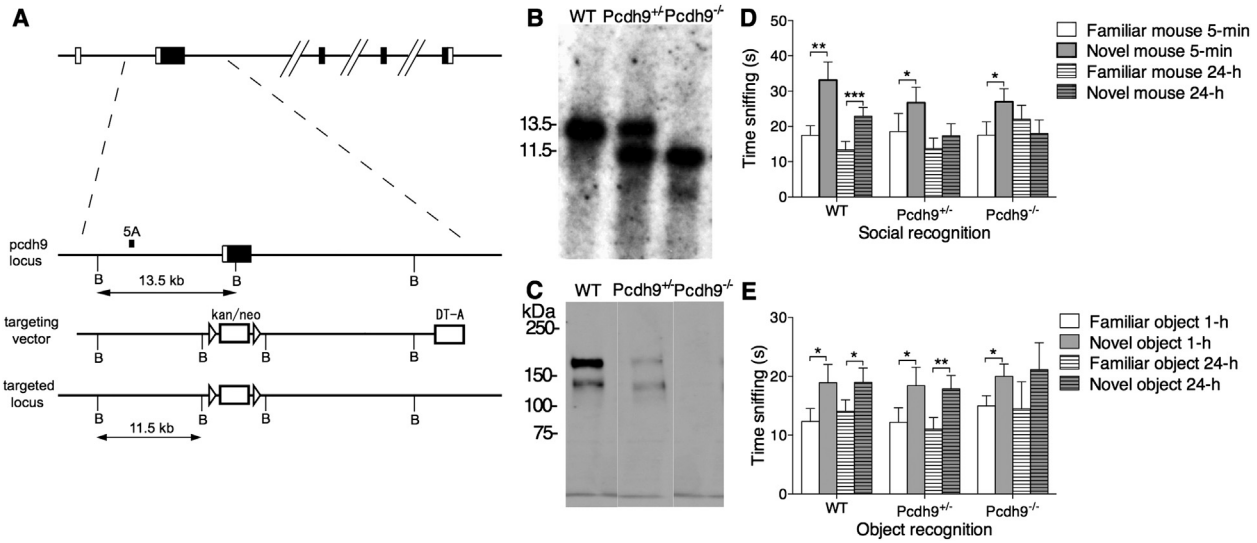

Figure 2. Generation of the *Pcdh9*-deficient mice and validation of quantitative trait locus phenotypes. **(A)** Strategy of homologous recombination for targeting of the *Pcdh9* gene. Locus and *Pcdh9*, target vector, and resulting target locus are indicated by restriction sites and positions of probes (5A, 3B, neo) for genotyping. H, Hind III; B, Bam H I; A, Apa I. **(B,C)** Southern **(B)** and Western blot **(C)** analysis to detect expression of *Pcdh9*. **(D,E)** Social and object recognition in wild-type (WT), heterozygous ($Pcdh9^{+/-}$), and knockout ($Pcdh9^{-/-}$) mice, analyzed as time spent sniffing the familiar versus the unknown social intruder or nonsocial object (n = 10 mice/genotype). Data are presented as means ± SEM; *$p < .05$; **$p < .01$; ***$p > .001$.

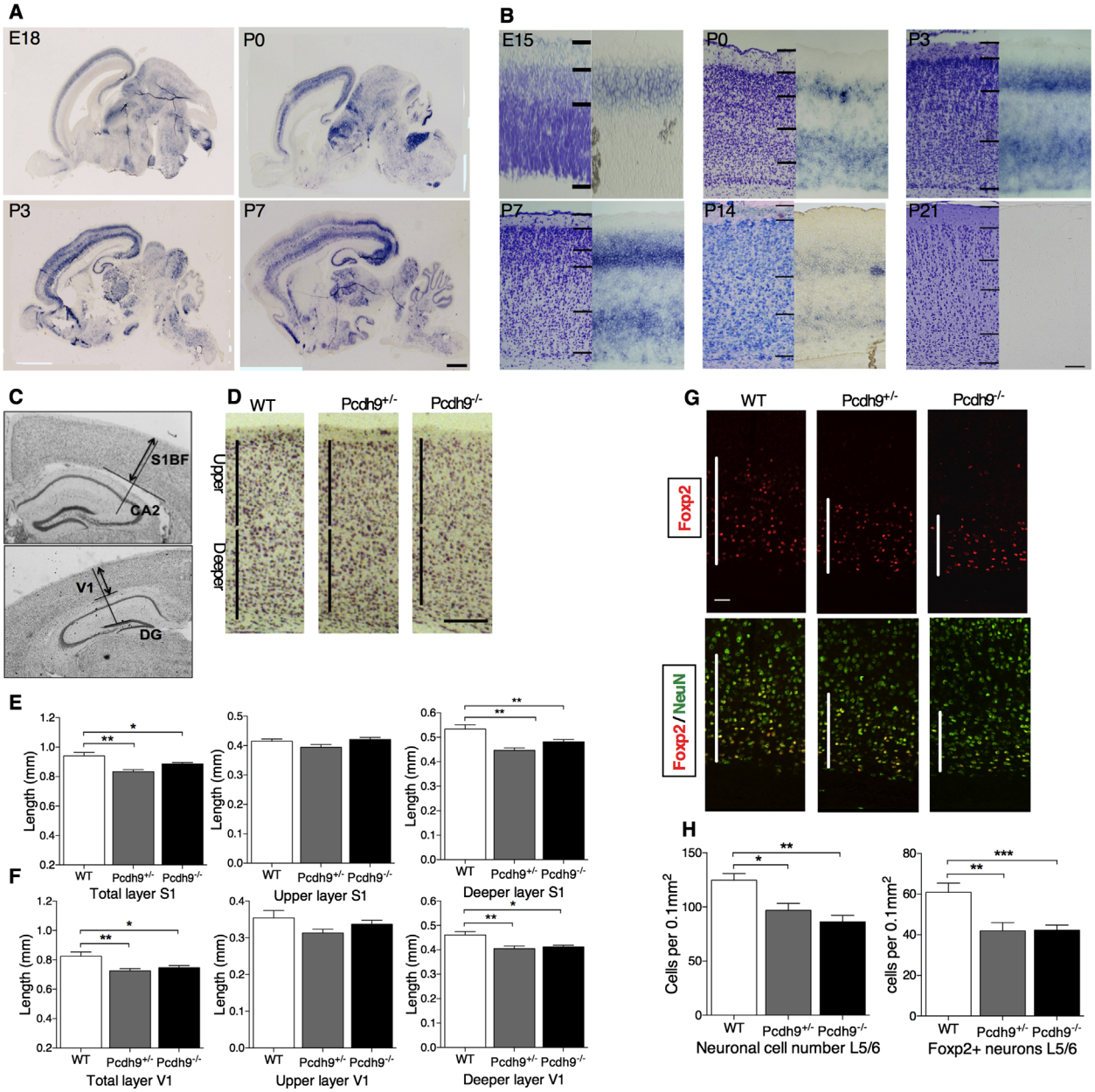

Figure 3. Spatiotemporal expression profile and structural changes in deep layers of the sensory cortices of *Pcdh9* mice. **(A)** *Pcdh9* expression in sagittal and coronal brain sections at different developmental stages. At postnatal day (P)7, high localized expression in posterior part of the parietal region and the anterior part of the occipital region and their innervating thalamic dorsal lateral geniculate and ventrobasal nuclei. Nissl staining (P7) lower right panel. Scale bar = 1 mm. **(B)** *Pcdh9* expression in layers of the occipital region of neocortices. Nissl staining is shown to the left, in situ signals to the right of each stage. Scale bar = 100 μm. **(C)** Detection of sensory cortex areas in cortex. For somatosensory cortex (primary somatosensory barrel cortex field [S1BF]), hippocampus cornu ammonis 2 (CA2) around bregma −1.70 mm area was used as a marker for detection. For visual cortex (primary visual cortex [V1]), hippocampus dentate gyrus (DG) around bregma −2.30 mm area was used. **(D)** Examples of Nissl stainings of the primary somatosensory cortex. Scale bar = 200 μm. **(E,F)** Quantitative analysis of cortical thickness in primary somatosensory (barrel) cortex (S1) **(E)**, visual cortex (V1) **(F)** ($n = 4$). **(G)** Expression of Foxp2 (red), a marker for deeper layer projection neurons, NeuN (green), a general neuronal marker, and merge (yellow). A narrower band of FoxP2+ cells in heterozygous ($Pcdh9^{+/-}$) and knockout ($Pcdh9^{-/-}$) versus wild-type (WT) mice is indicated ($n = 4$). Scale bar = 50 μm. **(H)** Quantitative analysis of neuronal cell number (NeuN) in deeper layers (L5/6) and quantitative analysis of number of Foxp2+ cell in deeper layers ($n = 4$ mice/genotype). Data are presented as means ± SEM; $^{*}p < .05$, $^{**}p < .01$, $^{***}p < .001$. E, embryonic day.

another species; a genetic mapping study associated *Pcdh9* with social behaviors in dogs (39,40). In view of the non-conserved nsSNP and its association with social behavior in different mammalian species, *Pcdh9* was the most promising candidate gene for further validation of its functional involvement in SRE and ASD.

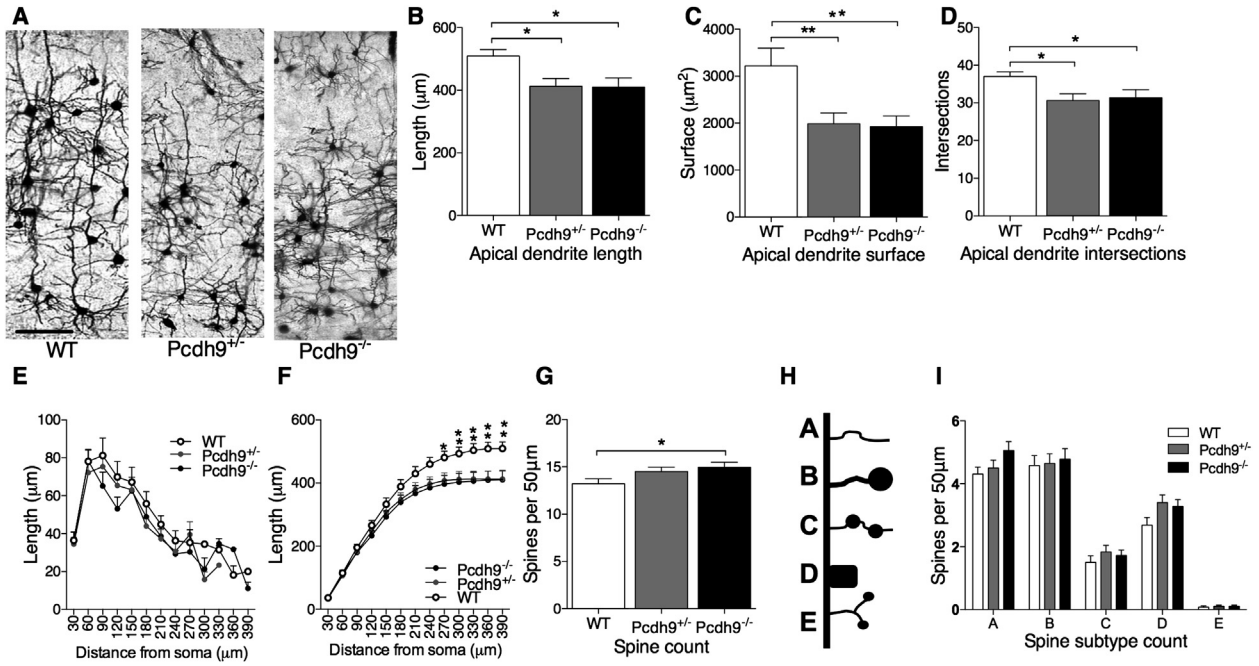

Figure 4. Reduced dendritic arborization and increased spine density in somatosensory cortex of *Pcdh9* mice. **(A)** Golgi staining of the somatosensory cortex. Scale bar = 50 μm. Note the disorientation and reduced complexity of dendritic arbors in deeper layers of *Pcdh9* mutant mice. **(B,C,D)** Quantitative analysis of average length **(B)**, surface **(C)**, and number of intersections (Sholl analysis) **(D)** of apical dendrite in L6 of primary somatosensory (barrel) cortex (n = 25 neurons from five mice for each genotype). **(E,F)** Quantitative analyses of segmental **(E)** and cumulative **(F)** apical dendrite length as a function from cell soma distance (Sholl analysis). **(G)** Quantitative analysis of spine density on apical dendrite segments from 2 × 25 μm segments of the first branch of the apical dendrite of L6 pyramidal neurons (n = 25 neurons from five mice for each genotype). **(H)** Examples of spine subtypes on apical dendrite segments. Subtypes ranging from immature (type A) to more mature (type D) and aberrant (type E) were characterized. **(I)** Quantitative analysis of spine subtypes on apical dendrite segments of Figure 5G. Data are presented as the mean ± SEM; *$p < .05$; **$p < .01$. WT, wild-type.

Validation of QTL Recognition Phenotypes in *Pcdh9*-Deficient Mice

We generated heterozygous (*Pcdh9*$^{1/2}$) (HZ) and homozygous (*Pcdh9*$^{2/2}$) knockout mice by replacing the whole second exon (Figure 2A–C; Table S2 in Supplement 1). In agreement with the results of the QTL analysis, we found intact SRE following the short-term 5-minute ITI and impaired SRE following the long-term 24-hour ITI in both *Pcdh9*$^{+/-}$ HZ and *Pcdh9*$^{-/-}$ KO mice, analyzed as actual time spent sniffing each nonsocial object or social intruder (Figure 2D). Importantly, the long-term SRE impairment in KO mice was confirmed in the laboratory in Osaka showing the robustness of this impairment (Figure S2 in Supplement 1). Similarly, the NORE capacity in KO mice was found to be intact after 1-hour ITI and impaired after 24-hour ITI, while NORE performance was unaffected in HZ mice after both ITIs (Figure 2E). The genotype effects on long-term SRE and NORE could not be explained by reduced initial exploration, as we did not observe genotype differences in the time spent sniffing of the initial familiar intruder and of the initial identical objects (data not shown). These results showed that KO mice recapitulated the SRE and NORE phenotype of the CSS14 mice and supported the involvement of *Pcdh9* in the regulation of long-term recognition.

Effects of *Pcdh9* Deletion on Sensory Cortical Architecture

To gain understanding of how *Pcdh9* loss of function reduces recognition capacity, we investigated the spatiotemporal expression of *Pcdh9* in mouse brain. We extended the existing analyses of *Pcdh9* expression (31,41–47) and found that *Pcdh9* was already expressed in several brain regions by embryonic day 18 (Figure 3A), with peak expression at postnatal day (P)7 in the somatosensory and visual cortices and its afferent thalamic nuclei (Figure 3A). Strong expression in the sensory cortical regions was mostly restricted to cortical layers 4 and 6 (Figure 3B). At P14, expression declined markedly to become nearly absent at P21. *Pcdh9* expression was also observed in the hippocampus, superior colliculus, and cerebellar cortex (Figure 3A). The specific spatiotemporal expression pattern indicated a developmental role in the emergence of functional circuitry and of sensory processing areas in particular.

To test the effect of *Pcdh9* deletion in expressed brain areas, we investigated hippocampus surface and cerebellar Purkinje cell numbers in *Pcdh9* KO mice. Both did not differ in *Pcdh9* KO, HZ, and wild-type (WT) mice (Figure S3 in Supplement 1). In primary somatosensory (S1) and visual V1 cortices (Figure 3C), we found a significant reduction in cortical thickness restricted to the deeper layers in both of HZ and KO versus WT mice (Figure 3D,E). Immunohistochemical analyses identified that this reduction in cortical thinning emerged with a reduced number of total neuron count (NeuN) and of Foxp2-positive (Figure 3F), a marker for deep cortical layer neurons (Figure 3G,H) (48). Consistent with the low *Pcdh9* messenger RNA expression in the motor cortex, the

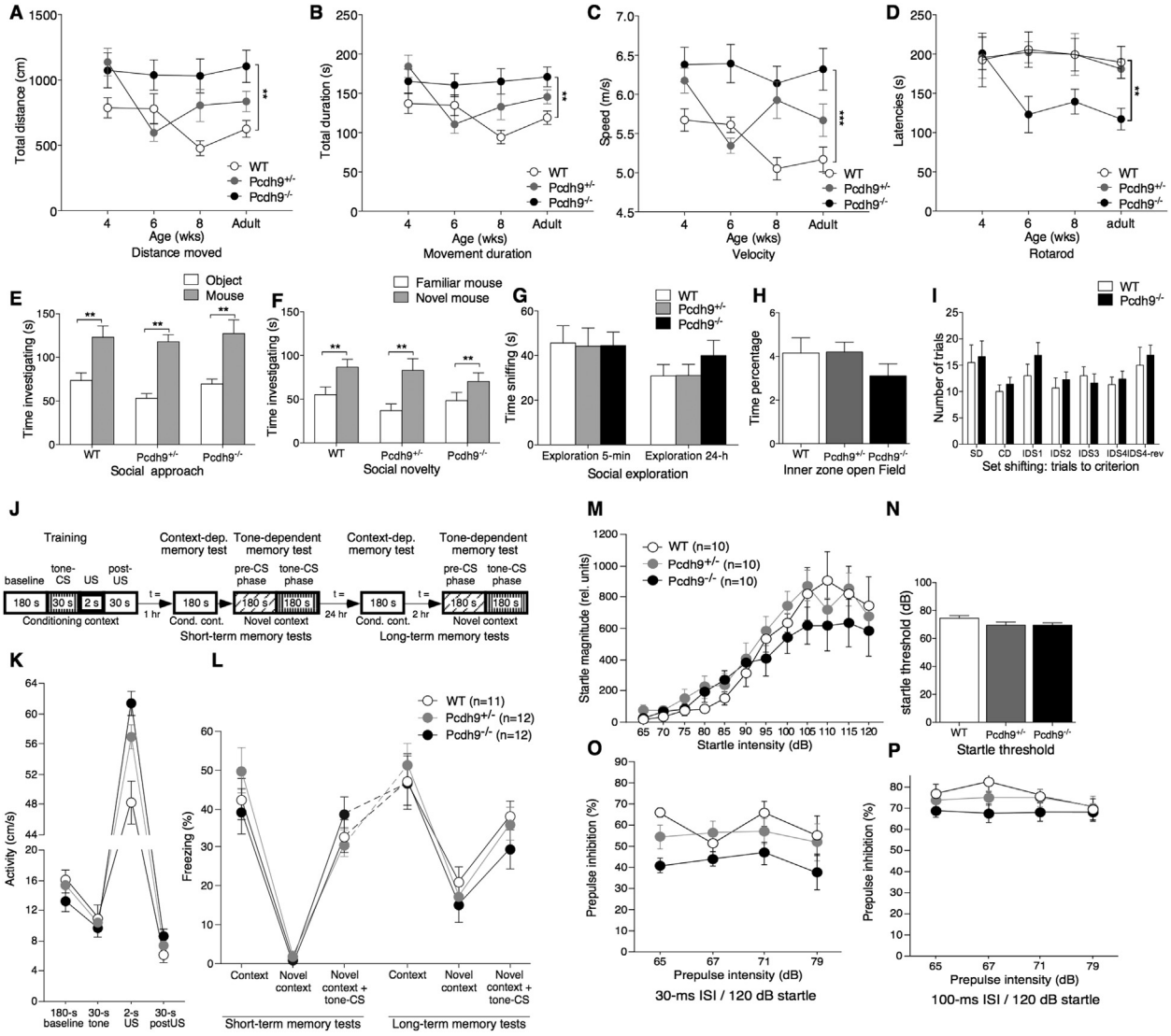

Figure 5. Developmental neurological and behavioral screening of *Pcdh9* mice. **(A–D)** Developmental trajectories from early adolescence until adulthood in wild-type (WT), *Pcdh9*$^{+/-}$, and *Pcdh9*$^{-/-}$ mice for distance moved **(A)**, movement duration **(B)**, movement velocity **(C)**, and latency to fall off the accelerating rotarod performance **(D)**. X axis represents the different time points of measurements (n = 10 mice/genotype). **(E,F)** Social approach as a function of the exploration of the cage with the novel mouse versus the empty cage **(E)** and social novelty preference as a function of exploration of the novel versus the familiar mouse **(F)** in the three-chamber task (n = 10 mice/genotype). **(G)** Social exploration in discrimination test as the total duration of social exploration test following 5-minute and 24-hour intertrial interval. **(H)** Open field anxiety as percentage of total time spent in inner zone of the field. **(I)** Behavioral flexibility measured by set shifting/reversal task. Y axis represents the number of errors made before criterion was reached. X axis represents the different subtasks: simple discrimination (SD), compound discrimination (CD), intradimensional shift I–IV (IDS I–IV), reversal of intradimensional shift IV (IDS-reversal) (n = 8-10 mice/genotype). **(J–L)** Fear conditioning performance as a function of genotype with *Pcdh9*-deficient (*Pcdh9*$^{-/-}$), heterozygous (*Pcdh9*$^{+/-}$), and wild-type mice (*Pcdh9*$^{+/+}$). Schematic presentation of the fear conditioning test sequence **(J)**. Training performance **(K)**. Short-term and long-term memory test performance **(L)**. **(M–P)** Startle results in *Pcdh9* mice. Startle magnitude as function of startle stimulus in all genotypes **(M)**. Startle threshold **(N)** and prepulse inhibition was tested with different prepulse intensities at 30-millisecond interstimulus interval (ISI) **(O)** and at 100-millisecond ISI **(P)**. Data are presented as means ± SEM; *$p < .05$, **$p < .01$, ***$p < .001$. CS, conditioned stimulus; cond. cont., conditioning context; dep., dependent; US, unconditioned stimulus.

thickness and cell numbers of the motor cortex layers were not altered in this region in HZ and KO mice (Figures S4A and S4B in Supplement 1).

To further study cortical architecture in deeper layers of S1, we analyzed dendrite morphology of pyramidal neurons in L6 using the Golgi-Cox impregnation method (Figure 4A). Sholl analysis confirmed a significant decrease in total apical dendrite length, surface, and number of intersections in HZ and KO mice (Figure 4B–D). This phenotype was not related to any particular segment distance from the cell soma (Figure 4E,F). Basal dendrite arbor length and surface were not significantly reduced (data not shown). Finally, we analyzed the type and number of spine segments of the primary branch of apical dendrites and found a significant increase in total spine number in *Pcdh9* KO

(Figure 4G). Spine subtype analysis revealed no difference in KO versus WT mice (Figure 4H,I). Thus, consistent with the strong messenger RNA expression of *Pcdh9* in deeper layers of the somatosensory cortex, these findings showed that *Pcdh9* deficiency caused reduced thickness of deeper layers in primary somatosensory cortex, which was associated with reduced dendritic arborization and complexity, increased spine density, and a reduction in the number of layer-specific pyramidal neurons.

Behavioral Phenotype of *Pcdh9*-Deficient Mice

To study the impact of *Pcdh9* deletion on behavioral development, we studied neurological and behavioral functions through an extended, partially longitudinal, test battery, the eSHIRPA (12), starting at 4 weeks of age and repeated at 6, 8, and 10 weeks of age. Deletion of one or both alleles of the *Pcdh9* gene did not cause any general health problems, differences in body weight, neurological effects, or gross morphological features across the different time points (Table S3 and Figure S5 in Supplement 1). Basic sensory properties were also intact, apart from one sensory measure in KO mice, i.e., touch-evoked biting. Locomotor assessments in the developmental screening revealed that KO, but not HZ, mice showed increased activity, velocity, and distance moved across all ages tested (Figures 5A–C) and impaired development of sensorimotor competence emerging from 6 weeks of age that were detected on the rotarod (Figure 5D).

WT and *Pcdh9* mutant mice were also tested in the three-chamber assay. The social approach test of this paradigm showed that all genotypes preferred to explore the cage with the mouse to the empty cage, indicating intact sociability and no social avoidance behavior (Figure 5E). In the second step of the three-chamber test, social novelty after a 5-minute interval was tested. This test showed that *Pcdh9* knockout mice had a significant preference for the chamber with the novel mouse versus that with the familiar mouse (Figure 5F). These three-chamber test findings were consistent with the intact short-term SRE performance of *Pcdh9* KO mice that were obtained from the social discrimination procedure (Figure 2E).

Locomotor and anxiety behavior were also investigated in the *Pcdh9* strain using an open field paradigm. No genotype differences were observed in total distance moved (Figure S6 in Supplement 1), indicating that at adult age no hyperactivity was indicated in contrast to what was observed in the eSHIRPA test during preadult stages. In addition, normal levels of anxiety-like behavior were observed by the lack of genotype differences in exploratory behavior determined by zone crossings in the open field (e.g., no genotype differences in levels of outer versus inner zone movements) (Figure 5H).

Next, we tested whether the single-trial recognition impairments were also upheld in multi-trial associative learning in an extensive set-shifting paradigm (49). Training with repeated training sessions indicated that WT and KO mice performed equally well on learning and memory of compound versus reward discrimination. Furthermore, KO mice managed the reversal-learning task, indicating no effect of deletion of *Pcdh9* on cognitive flexibility (Figure 5I). Memory and learning were further tested in single-trial fear conditioning to contextual and explicit cues (Figure 5J). Both short-term (1-hour) and long-term (24-hour) memory tests yielded similar performances, indicating no emotional learning deficit and thus unaffected fear acquisition and consolidation for hippocampus-dependent contextual and hippocampus-independent memory functions in *Pcdh9*-deficient mice (Figure 5K,L) (Supplement 1).

Finally, we tested sensory processing capabilities through startle experiments including sensory gating in a PPI test (Figure 5M–P) (Supplement 1). Startle measurements indicated no difference in the startle intensity and threshold (Figure 5M, N), suggesting no difference in anxiety-like behavior and no auditory impairment, extending the auditory fear conditioning and open field anxiety readouts. Measurement of sensory gating showed lower prepulse inhibition, specifically at 30-millisecond interstimulus interval, indicated a sensorimotor gating deficit in KO mice (Figure 5O). Experiments with 100-millisecond interstimulus interval (Figure 5P) indicated no significant genotype effect on PPI (Figure 5P).

In summary, the recognition impairments in KO mice were not associated with reduced perception, social exploration, social approach behavior, memory, and behavioral inflexibility. The behavioral phenotype of KO mice was characterized by hyperactivity, reduced touch-evoked biting, reduced sensorimotor competence, and impaired sensory gating. In comparison with KO mice, HZ mice displayed only impaired long-term SRE and no changes in any of the other investigated parameters.

DISCUSSION

We show that quantitative genetic analysis of basic mouse behaviors can uncover genotypes related to subtle behavioral and neurodevelopmental disruptions of relevance to human psychiatric disorders. By using chromosome substitution strains, we identified *Pcdh9* as an interesting candidate previously associated with ASD (34–38) and social behavioral phenotypes in dogs (39,40). After generation of *Pcdh9* KO mice, we confirmed specific effects of *Pcdh9* deficiency on long-term NORE and SRE, which were recapitulated in a second independent laboratory. Subsequently, we performed an anatomical, neurological, and behavioral characterization of *Pcdh9* KO mice to gain understanding of the impact of this gene on behavioral development and to test various components associated with recognition capacities.

Subsequent series of intradimensional set-shifting experiments revealed that long-term memory was equally established in KO and WT mice after multi-trial discrimination learning. The results of the fear memory tests also indicated no emotional short-term and long-term learning deficits, as unaffected fear acquisition and consolidation for hippocampus-dependent contextual and hippocampus-independent cued memory functions were found (50). The developmental screening indicated intact basic neurological reflexes and sensory perception, apart from reduced touch-evoked biting in KO mice. Interestingly, two other tests showed impairments relating to sensorimotor behaviors; the rotarod test indicated reduced sensorimotor competence and the PPI test indicated sensory gating impairments. Together,

these results show that the long-term recognition defects in *Pcdh9*-deficient mice are not caused by inadequate sensory perception, sociability, or encoding (no deficient short-term) and are also not associated with downstream memory consolidation impairment. We hypothesize that the combination of reduced long-term recognition with sensory gating and sensorimotor competence indicates a discrete impact of *Pcdh9* deletion on higher order sensory processing with very specific behavioral consequences. Interestingly, (proto)cadherins are known to be involved in the development of functional cortical circuitry morphology (44,51,52), which has been attributed to their homophilic binding properties in dendritic outgrowth and synapse contact formation (53–57). Such a function seems consistent with the specific spatiotemporal expression pattern in sensory systems and the observed morphological changes in the primary somatosensory and visual cortex. Social and object recognition depend on proper processing of (social and nonsocial) sensory stimuli followed by encoding and memory consolidation. Interestingly, primary sensory cortices have been explicitly implicated in processing and storage of specific sensory experiences (58,59) and perceptual awareness of sensations, an important upstream function before hippocampal involvement in encoding and consolidation of more complex associations, as in contextual fear conditioning. Nonetheless, our hypothesis is mostly based upon behavioral and developmental findings and requires experimental support from additional (mechanistic) studies.

Our findings have translational value as sensory processing disorders are increasingly being implicated in neurodevelopmental disorders (60–62). In particular, PPI defects are generally regarded as a schizophrenia-like phenotype (63,64) but are also reported in genetic mouse models for ASD risk genes (65,66) and in adult humans with ASD (8). Consistently, behavioral symptoms relating to lower and higher order sensory processing abnormalities are frequently reported in ASD (60,67,68) and have been added to the diagnostic criteria for ASD in the Diagnostic and Statistical Manual of Mental Disorders (69). In addition, sensory processing disorders are also increasingly recognized as an independent clinical entity (62), which may relate to the phenotypic profile in the *Pcdh9* KO mice.

In summary, quantitative analysis of basic mouse behavior uncovered a role for *Pcdh9* in specific cognitive functions required for long-term recognition. This role is supported by the involvement of *Pcdh9* in sensory cortex development and the effect of its deletion on sensorimotor behaviors. Our study underscores the strength of forward genetic mapping in mice to disentangle functional contributions of genetic variation to aberrant behavioral development.

ACKNOWLEDGMENTS AND DISCLOSURES

These studies were supported by a ZonMW VIDI Grant (91786327) from The Netherlands Organization for Scientific Research and funding by European Autism Interventions - A Multicentre Study for Developing New Medications (EU-AIMS) to Dr. Martien J. Kas and by the Dobberke Grant from the Dr. J.L. Dobberke Foundation for Comparative Psychology to Dr. Hilgo Bruining. The research of European Autism Interventions - A Multicentre Study for Developing New Medications (EU-AIMS) receives support from the Innovative Medicines Initiative Joint Undertaking under Grant agreement number 115300, resources of which are composed of financial contributions from the European Union's Seventh Framework Programme (FP7/2007-2013), from the European Federation of Pharmaceutical Industries and Associations companies in-kind contributions, and from Autism Speaks. Dr. Asami Oguro-Ando is supported by the Canon Foundation (Europe Research Fellowship).

Dr. Hilgo Bruining was funded by the Dobberke Grant from the Dr. J.L. Dobberke Foundation for Comparative Psychology.

Dr. Asami Oguro-Ando reports having received research funding from the Canon Foundation (Europe Research Fellowship).

Dr. Nobuhiko Yamamoto reports having received research funding from Grant-in-Aid for Scientific Research on Innovative Areas Mesoscopic Neurocircuitry (No. 23115102) from the Ministry of Education, Culture, Sports, Science and Technology of Japan and Grants-in-Aid for Scientific Research (No. 20300110 and No. 20021018) from the Ministry of Education, Culture, Sports, Science and Technology of Japan.

Dr. Martien J. Kas reports having received research funding from a ZonMW VIDI Grant (91786327) from The Netherlands Organization for Scientific Research and funding from European Autism Interventions - A Multicentre Study for Developing New Medications (EU-AIMS). The research of European Autism Interventions - A Multicentre Study for Developing New Medications (EU-AIMS) receives support from the Innovative Medicines Initiative Joint Undertaking under Grant agreement number 115300, resources of which are composed of financial contributions from the European Union's Seventh Framework Programme C (FP7/2007-2013), from the European Federation of Pharmaceutical Industries and Associations companies in-kind contributions, and Autism Speaks.

All other authors report no biomedical financial interests or potential conflicts of interest.

ARTICLE INFORMATION

From the Department of Translational Neuroscience (HB, AO-A, HMvS, GA, HO, LT, LJN, JPHB, MJK) and Department of Psychiatry (HB, RSK, HvE), Brain Center Rudolf Magnus, University Medical Center Utrecht, Utrecht, The Netherlands; Neuroscience Laboratories (AM, NY), Graduate School of Frontier Biosciences, Osaka University, Osaka, Japan; Center for Neurogenomics and Cognitive Research (OS), Neuroscience Campus Amsterdam, VU University Amsterdam, and Sylics (Synaptologics BV) (BK), Amsterdam, The Netherlands; Division of Animal Welfare & Laboratory Animal Science (HAvL), Department of Animals in Science and Society, Program Emotion and Cognition, Faculty of Veterinary Medicine, Utrecht University, The Netherlands; and KOKORO-Biology Group (TY, RK), Laboratories for Integrated Biology, Graduate School of Frontier Biosciences, Osaka University, Osaka, Japan.

Authors HB, AM, and AO-A contributed equally to this work.

Address correspondence to Martien Kas, Ph.D., Rudolf Magnus Institute of Neuroscience, Department of Translational Neuroscience, Utrecht, The Brain Center Rudolf Magnus, Heidelberglaan 100, Utrecht 3584CX, Netherlands; E-mail: m.j.h.kas@umcutrecht.nl.

Received May 30, 2014; revised Jan 9, 2015; accepted Jan 13, 2015.

Supplementary material cited in this article is available online at http://dx.doi.org/10.1016/j.biopsych.2015.01.017.

REFERENCES

1. Abrahams BS, Geschwind DH (2010): Connecting genes to brain in the autism spectrum disorders. Arch Neurol 67:395–399.
2. Insel TR (2010): Rethinking schizophrenia. Nature 468:187–193.
3. Meyer-Lindenberg A, Weinberger DR (2006): Intermediate phenotypes and genetic mechanisms of psychiatric disorders. Nat Rev Neurosci 7: 818–827.
4. Flint J, Timpson N, Munafo M (2014): Assessing the utility of intermediate phenotypes for genetic mapping of psychiatric disease. Trends Neurosci 37:733–741.
5. Donaldson ZR, Hen R (2015): From psychiatric disorders to animal models: A bidirectional and dimensional approach. Biol Psychiatry 77: 15–21.

6. Kas MJ, Fernandes C, Schalkwyk LC, Collier DA (2007): Genetics of behavioural domains across the neuropsychiatric spectrum; of mice and men. Mol Psychiatry 12:324–330.
7. Berry RJ, Bronson FH (1992): Life history and bioeconomy of the house mouse. Biol Rev Camb Philos Soc 67:519–550.
8. Young LJ (2002): The neurobiology of social recognition, approach, and avoidance. Biol Psychiatry 51:18–26.
9. Engelmann M, Hadicke J, Noack J (2011): Testing declarative memory in laboratory rats and mice using the nonconditioned social discrimination procedure. Nat Protoc 6:1152–1162.
10. Engelmann M, Wotjak CT, Landgraf R (1995): Social discrimination procedure: An alternative method to investigate juvenile recognition abilities in rats. Physiol Behav 58:315–321.
11. Engelmann M (2009): Competition between two memory traces for long-term recognition memory. Neurobiol Learn Mem 91:58–65.
12. Molenhuis RT, de Visser L, Bruining H, Kas MJ (2014): Enhancing the value of psychiatric mouse models; differential expression of developmental behavioral and cognitive profiles in four inbred strains of mice. Eur Neuropsychopharmacol 24:945–954.
13. Kas MJ, de Mooij-van Malsen JG, de Krom M, van Gassen KL, van Lith HA, Olivier B, *et al*. (2009): High-resolution genetic mapping of mammalian motor activity levels in mice. Genes Brain Behav 8:13–22.
14. Cox A, Ackert-Bicknell CL, Dumont BL, Ding Y, Bell JT, Brockmann GA, *et al*. (2009): A new standard genetic map for the laboratory mouse. Genetics 182:1335–1344.
15. Broman KW, Wu H, Sen S, Churchill GA (2003): R/qtl: QTL mapping in experimental crosses. Bioinformatics 19:889–890.
16. Losh M, Adolphs R, Poe MD, Couture S, Penn D, Baranek GT, Piven J (2009): Neuropsychological profile of autism and the broad autism phenotype. Arch Gen Psychiatry 66:518–526.
17. Yagi T, Tokunaga T, Furuta Y, Nada S, Yoshida M, Tsukada T, *et al*. (1993): A novel ES cell line, TT2, with high germline-differentiating potency. Anal Biochem 214:70–76.
18. Rogers DC, Jones DN, Nelson PR, Jones CM, Quilter CA, Robinson TL, Hagan JJ (1999): Use of SHIRPA and discriminant analysis to characterise marked differences in the behavioural phenotype of six inbred mouse strains. Behav Brain Res 105:207–217.
19. Lalonde R, Dumont M, Staufenbiel M, Strazielle C (2005): Neurobehavioral characterization of APP23 transgenic mice with the SHIRPA primary screen. Behav Brain Res 157:91–98.
20. Nadler JJ, Moy SS, Dold G, Trang D, Simmons N, Perez A, *et al*. (2004): Automated apparatus for quantitation of social approach behaviors in mice. Genes Brain Behav 3:303–314.
21. Misane I, Kruis A, Pieneman AW, Ogren SO, Stiedl O (2013): GABA(A) receptor activation in the CA1 area of the dorsal hippocampus impairs consolidation of conditioned contextual fear in C57BL/6J mice. Behav Brain Res 238:160–169.
22. Nadeau JH, Singer JB, Matin A, Lander ES (2000): Analysing complex genetic traits with chromosome substitution strains. Nat Genet 24:221–225.
23. de Mooij-van Malsen AJ, van Lith HA, Oppelaar H, Hendriks J, de Wit M, Kostrzewa E, *et al*. (2009): Interspecies trait genetics reveals association of Adcy8 with mouse avoidance behavior and a human mood disorder. Biol Psychiatry 66:1123–1130.
24. Krewson TD, Supelak PJ, Hill AE, Singer JB, Lander ES, Nadeau JH, Palmert MR (2004): Chromosomes 6 and 13 harbor genes that regulate pubertal timing in mouse chromosome substitution strains. Endocrinology 145:4447–4451.
25. Singer JB, Hill AE, Burrage LC, Olszens KR, Song J, Justice M, *et al*. (2004): Genetic dissection of complex traits with chromosome substitution strains of mice. Science 304:445–448.
26. Winawer MR, Gildersleeve SS, Phillips AG, Rabinowitz D, Palmer AA (2011): Mapping a mouse limbic seizure susceptibility locus on chromosome 10. Epilepsia 52:2076–2083.
27. Redies C (2000): Cadherins in the central nervous system. Prog Neurobiol 61:611–648.
28. Takeichi M (2007): The cadherin superfamily in neuronal connections and interactions. Nat Rev Neurosci 8:11–20.
29. Kahr I, Vandepoele K, van Roy F (2013): Delta-protocadherins in health and disease. Prog Mol Biol Transl Sci 116:169–192.
30. Redies C, Vanhalst K, Roy F (2005): delta-Protocadherins: Unique structures and functions. Cell Mol Life Sci 62:2840–2852.
31. Vanhalst K, Kools P, Staes K, van Roy F, Redies C (2005): delta-Protocadherins: A gene family expressed differentially in the mouse brain. Cell Mol Life Sci 62:1247–1259.
32. Kim SY, Yasuda S, Tanaka H, Yamagata K, Kim H (2011): Non-clustered protocadherin. Cell Adh Migr 5:97–105.
33. Redies C, Hertel N, Hubner CA (2012): Cadherins and neuropsychiatric disorders. Brain Res 1470:130–144.
34. Bucan M, Abrahams BS, Wang K, Glessner JT, Herman EI, Sonnenblick LI, *et al*. (2009): Genome-wide analyses of exonic copy number variants in a family-based study point to novel autism susceptibility genes. PLoS Genet 5:e1000536.
35. Girirajan S, Dennis MY, Baker C, Malig M, Coe BP, Campbell CD, *et al*. (2013): Refinement and discovery of new hotspots of copy-number variation associated with autism spectrum disorder. Am J Hum Genet 92:221–237.
36. Leblond CS, Heinrich J, Delorme R, Proepper C, Betancur C, Huguet G, *et al*. (2012): Genetic and functional analyses of SHANK2 mutations suggest a multiple hit model of autism spectrum disorders. PLoS Genet 8:e1002521.
37. Luo R, Sanders SJ, Tian Y, Voineagu I, Huang N, Chu SH, *et al*. (2012): Genome-wide transcriptome profiling reveals the functional impact of rare de novo and recurrent CNVs in autism spectrum disorders. Am J Hum Genet 91:38–55.
38. Marshall CR, Noor A, Vincent JB, Lionel AC, Feuk L, Skaug J, *et al*. (2008): Structural variation of chromosomes in autism spectrum disorder. Am J Hum Genet 82:477–488.
39. Chase K, Jones P, Martin A, Ostrander EA, Lark KG (2009): Genetic mapping of fixed phenotypes: Disease frequency as a breed characteristic. J Hered 100(suppl 1):S37–S41.
40. Starling MJ, Branson N, Thomson PC, McGreevy PD (2013): Age, sex and reproductive status affect boldness in dogs. Vet J 197:868–872.
41. Blevins CJ, Emond MR, Biswas S, Jontes JD (2011): Differential expression, alternative splicing, and adhesive properties of the zebrafish delta1-protocadherins. Neuroscience 199:523–534.
42. Kim SY, Chung HS, Sun W, Kim H (2007): Spatiotemporal expression pattern of non-clustered protocadherin family members in the developing rat brain. Neuroscience 147:996–1021.
43. Kim SY, Mo JW, Han S, Choi SY, Han SB, Moon BH, *et al*. (2010): The expression of non-clustered protocadherins in adult rat hippocampal formation and the connecting brain regions. Neuroscience 170: 189–199.
44. Krishna K, Nuernberger M, Weth F, Redies C (2009): Layer-specific expression of multiple cadherins in the developing visual cortex (V1) of the ferret. Cereb Cortex 19:388–401.
45. Lin J, Wang C, Redies C (2013): Expression of multiple delta-protocadherins during feather bud formation. Gene Expr Patterns 13: 57–65.
46. Liu Q, Chen Y, Pan JJ, Murakami T (2009): Expression of protocadherin-9 and protocadherin-17 in the nervous system of the embryonic zebrafish. Gene Expr Patterns 9:490–496.
47. Redies C, Neudert F, Lin J (2011): Cadherins in cerebellar development: Translation of embryonic patterning into mature functional compartmentalization. Cerebellum 10:393–408.
48. Molyneaux BJ, Arlotta P, Menezes JR, Macklis JD (2007): Neuronal subtype specification in the cerebral cortex. Nat Rev Neurosci 8: 427–437.
49. Bissonette GB, Martins GJ, Franz TM, Harper ES, Schoenbaum G, Powell EM (2008): Double dissociation of the effects of medial and orbital prefrontal cortical lesions on attentional and affective shifts in mice. J Neurosci 28:11124–11130.
50. Stiedl O, Birkenfeld K, Palve M, Spiess J (2000): Impairment of conditioned contextual fear of C57BL/6J mice by intracerebral injections of the NMDA receptor antagonist APV. Behav Brain Res 116:157–168.
51. Krishna KK, Hertel N, Redies C (2011): Cadherin expression in the somatosensory cortex: Evidence for a combinatorial molecular code at the single-cell level. Neuroscience 175:37–48.

52. Rakic P, Caviness VS Jr (1995): Cortical development: View from neurological mutants two decades later. Neuron 14:1101–1104.
53. Gao FB, Kohwi M, Brenman JE, Jan LY, Jan YN (2000): Control of dendritic field formation in Drosophila: The roles of flamingo and competition between homologous neurons. Neuron 28:91–101.
54. Lefebvre JL, Kostadinov D, Chen WV, Maniatis T, Sanes JR (2012): Protocadherins mediate dendritic self-avoidance in the mammalian nervous system. Nature 488:517–521.
55. Piper M, Dwivedy A, Leung L, Bradley RS, Holt CE (2008): NF-protocadherin and TAF1 regulate retinal axon initiation and elongation in vivo. J Neurosci 28:100–105.
56. Shima Y, Kengaku M, Hirano T, Takeichi M, Uemura T (2004): Regulation of dendritic maintenance and growth by a mammalian 7-pass transmembrane cadherin. Dev Cell 7:205–216.
57. Yasuda S, Tanaka H, Sugiura H, Okamura K, Sakaguchi T, Tran U, *et al*. (2007): Activity-induced protocadherin arcadlin regulates dendritic spine number by triggering N-cadherin endocytosis via TAO2-beta and p38 MAP kinases. Neuron 56:456–471.
58. Weinberger NM (2004): Specific long-term memory traces in primary auditory cortex. Nat Rev Neurosci 5:279–290.
59. Headley DB, Weinberger NM (2013): Relational associative learning induces cross-modal plasticity in early visual cortex [published online ahead of print November 24]. Cereb Cortex.
60. Ben-Sasson A, Hen L, Fluss R, Cermak SA, Engel-Yeger B, Gal E (2009): A meta-analysis of sensory modulation symptoms in individuals with autism spectrum disorders. J Autism Dev Disord 39:1–11.
61. Brown C, Cromwell RL, Filion D, Dunn W, Tollefson N (2002): Sensory processing in schizophrenia: Missing and avoiding information. Schizophr Res 55:187–195.
62. Miller LJ, Nielsen DM, Schoen SA, Brett-Green BA (2009): Perspectives on sensory processing disorder: A call for translational research. Front Integr Neurosci 3:22.
63. Swerdlow NR, Braff DL, Geyer MA (2000): Animal models of deficient sensorimotor gating: What we know, what we think we know, and what we hope to know soon. Behav Pharmacol 11:185–204.
64. Braff DL, Grillon C, Geyer MA (1992): Gating and habituation of the startle reflex in schizophrenic patients. Arch Gen Psychiatry 49:206–215.
65. Aldinger KA, Plummer JT, Qiu S, Levitt P (2011): SnapShot: Genetics of autism. Neuron 72:418–8.e1.
66. Bacon C, Schneider M, Le Magueresse C, Froehlich H, Sticht C, Gluch C, *et al*. (2014): Brain-specific Foxp1 deletion impairs neuronal development and causes autistic-like behaviour [published online ahead of print September 30]. Mol Psychiatry.
67. Brown T, Leo M, Austin DW (2008): Discriminant validity of the Sensory Profile in Australian children with autism spectrum disorder. Phys Occup Ther Pediatr 28:253–266.
68. Rogers SJ, Ozonoff S (2005): Annotation: What do we know about sensory dysfunction in autism? A critical review of the empirical evidence. J Child Psychol Psychiatry 46:1255–1268.
69. Mandy WP, Charman T, Skuse DH (2012): Testing the construct validity of proposed criteria for DSM-5 autism spectrum disorder. J Am Acad Child Adolesc Psychiatry 51:41–50.